Analysis of the C260 brass after mechanical forming and annealing

Douglas Luiz da Cruz [1]*, Matheus José Cunha de Oliveira [2], Cristian Pohl Meinhardt [3]

[1] douglascruzjf@gmail.com , [2] matheus.oliveira@ifsudestemg.edu.br. Instituto Federal de Educação, Ciência e Tecnologia do Sudeste de Minas Gerais (IF SUDESTE MG), Juiz de Fora, MG, Brasil.
[3] cristianmeinhardt@unipampa.edu.br. Universidade Federal do Pampa (UNIPAMPA), Alegrete, RS, Brasil.
* autor correspondente

Abstract
Copper alloys such as brass are highly used in the most varied branches of industry due to their characteristics such as corrosion resistance and formability. Among the processes used to manufacture parts made with such alloys, processes such as deep stamping or inlaying and stretching stand out. Such mechanical conformation processes require the use of thermal treatments such as annealing, in order to obtain specific properties in the resulting material. Therefore, this work aimed to evaluate the mechanical behavior of C260 brass when subjected to mechanical shaping (blanking and stretching) and annealing heat treatment. For this, a script clipping of an ammunition component was used, taking samples step by step including the raw material and dividing them into different regions, when in the shape of a cup, to understand the processes. Metallographic tests were carried out where, along with the microstructural evaluation, it was possible to determine grain size in addition to the Vickers microhardness. The grain size data were treated statistically, thus making it possible to judge the significance of each microstructure alteration. Thus, it was possible to observe that the mechanical forming steps actually hardened the material with an increase in hardness, unlike the annealing. However, a difference in behavior was noted in two different regions of the cups, where the wall region showed significant microstructural variations as well as its hardness, unlike the bottom region. The percentage of cold work parameters was identified as responsible for this difference both for recrystallizations to occur, as well as for the resulting microstructure and consequent hardness. The evaluation of the data referring to the raw material confirmed the fulfillment of its technical requirements.
Keywords: copper alloy; heat treatment; metallurgy; microstructure.

Análise do latão C260 após conformações mecânicas e recozimento

Resumo
Ligas de cobre como o latão são muito utilizadas nos mais variados ramos da indústria devido às suas características como resistência à corrosão e conformabilidade. Dentre os processos utilizados para a fabricação de peças fabricadas com essas ligas, destacam-se processos como estampagem profunda ou embutimento e estiramento. Tais processos de conformação mecânica requerem a utilização de tratamentos térmicos como o recozimento, a fim de obter propriedades específicas no material resultante. Portanto, este trabalho teve como objetivo avaliar o comportamento mecânico do latão C260 quando submetido a tratamento térmico de conformação mecânica (embutimento e estiramento) e recozimento. Para isso, foi utilizado um recorte de roteiro de um componente de munição, retirando passo a passo amostras incluindo a matéria-prima e dividindo-as em diferentes regiões, quando em formato de copo, para entender os processos. Foram realizados ensaios metalográficos onde junto com a avaliação microestrutural foi possível determinar o tamanho dos grãos além do ensaio de microdureza Vickers. Os dados de tamanho de grão foram tratados estatisticamente, possibilitando julgar a significância de cada alteração microestrutural. Assim, foi possível observar que as etapas de conformação mecânica realmente endureceram o material com aumento de dureza, diferentemente do recozimento. Porém, foi notada diferença de comportamento em duas regiões distintas dos copos, onde a região da parede apresentou variações microestruturais significativas, bem como sua dureza,

diferentemente da região do fundo. O parâmetro percentual de trabalho a frio foi identificado como responsável por esta diferença tanto para que ocorram recristalizações, quanto para a microestrutura resultante e consequente dureza. A avaliação dos dados referentes à matéria-prima confirmou o atendimento aos seus requisitos técnicos.
Palavras-chave: liga de cobre; metalurgia; microestrutura; tratamento térmico.

1 Introduction

Blanking is a sheet metal forming process characterized by a punch moving against another tool called a matrix containing the sheet metal. The geometry of the punch/die set is responsible for the new shape of the sheet metal (Hirt *et al*., 2005).

Brass is a copper–zinc (Cu–Zn) solid-solution alloy that combines the corrosion resistance and formability of copper with higher mechanical strength. It is widely used to manufacture complex shapes, for example by deep drawing, because it hardens slowly, tolerates stress well, and fractures only at high strains. (Brooks, 1982). In this way, it is noted the great importance of this alloy in the metalworking industry. The aforementioned characteristics, together with its good appearance, make brass used in several areas, such as decoration, electrical, automotive, military, civil construction, oil and gas (Barbosa, 2014).

The deformation processes used to obtain certain application characteristics in the final product require the use of a heat treatment. This aims to restore the material's physical-mechanical properties to their previous levels. Such treatment is called annealing. The metallurgical phenomena characteristic of the annealing of metallic alloys and their relationship with the microstructure of the deformed metal have been objects of study for many years (Moreira, 2015).

The present work focuses its analysis on a specific brass alloy, the binary brass C260, also known as "cartridge brass" due to its well-known application in the manufacture of ammunition components. It is a single-phase alloy, therefore, its microstructure consists only of α phase (copper with zinc in solid solution), very suitable for stamping processes due to its good mechanical resistance and excellent ductility. The proposed analysis seeks to elucidate the behavior of Cu-Zn 30 brass, as it is also known, through mechanical forming and heat treatment in a cutout of the manufacture script of an ammunition component.

2 Bibliographic review

Stamping is a set of various operations carried out on blank metal sheets, which aim to transform them geometrically, resulting in folds, cavities, protrusions, wedges and holes. Such deformations occur in the solid state, so that the material flows in a plastic regime. One of the positive points of stamping is the reduced waste and low generation of raw material scraps.

Plastic deformation, generally cold, is carried out using stamping presses equipped with devices called stamps or matrices. As a result of the characteristics of this sheet metal forming process, different ways of working have been developed over the years, bringing together specialists from each process for their respective application. Along with this diversification of methods, there are several peculiar parameters of each process. Such as: tooling angles and radii, financing, operating speed, roughness and strength, in addition to the physical-mechanical properties of the raw material used in the process.

Inlay or deep stamping is a stamping process used to transform flat sheets into three-dimensional and deep parts, of different shapes, such as cups, pans, capsules, car body components and metal packaging in general. The tooling used in these operations is called a stamp, and consists of a punch, a matrix and a holder called a plate press. During deep drawing, a force is exerted on the central region of the blank, forcing it towards the matrix cavity and pulling the flap region in the same direction, which results in a gradual reduction in the circumference of the disc in this region. This effort generates tensile and compressive tensions in several regions. Tensions act in the flap region, which touches the concentric circles to the central region, called circumferential compression and which tend to wrinkle the sheet. To avoid this, the plate press must exert a compressive stress, called holding pressure. The holding pressure should only be necessary to avoid

the appearance of wrinkles, thus allowing the movement of the disc flap towards the central region. Stretch forming is characterized by a state of biaxial traction, where traction forces are applied in order to stretch the material over a tool or block (die), thus defining the contour of the part and also a reduction in the thickness of the material. The spring effect is almost completely eliminated due to a higher percentage of plastic deformation caused by the tensile force, thus reducing residual stresses. However, only in materials with high ductility values, can large stretching deformations be obtained due to the predominance of tensile stresses (Grigoras *et al*., 2024).

The stresses generated in various manufacturing processes such as: casting, mechanical forming and even machining imply changes in the structures of the materials, modifying the mechanical properties of the materials that pass in this way, not always corresponding to the application requirements of the manufactured parts (Merayo *et al*., 2021). Therefore, there is a need to subject them to heat treatments that aim to readapt such properties, which can be considered the most common method of achieving such feats.

The term annealing is used, in a generic way, to describe a set of heat treatments carried out with the aim, in short, of relieving or removing pre-existing stresses; decrease hardness and improve ductility and toughness; and/or produce a specific microstructure. Basically it consists of heating the metal to a certain temperature, maintaining this temperature for a certain time known as "soaking" time and cooling the material to room temperature. The importance of controlling time in this heat treatment is extremely important considering that there are temperature gradients during heating and cooling in the material. Large rates of temperature variation can lead to warping or even cracking. The actual annealing time must be estimated in a way that allows for all necessary transformations to occur. Temperature is another very important parameter; which can accelerate annealing by increasing it, taking into account the diffusion processes normally involved (Birch *et al*., 2024).

Popularly known as "cartridge brass", the C260 single-phase copper alloy has a yellowish color and is highly recommended for various forming processes, particularly stamping and deep drawing, as it presents the most favorable combination between mechanical strength and ductility. Depending on the environment in which it is being used, it may present dezincification problems (Barbosa, 2014). In addition to the manufacture of ammunition components, Brass UNS C26000, as it is commercially known, has other diverse applications, such as: radiator cores and tanks, lamp fixtures, latches, locks, hinges, plumbing accessories, pins, rivets (ASM, 1992). Thus, this work aimed to demonstrate the mechanical behavior and microstructure characterization of the C260 brass alloy beneath the effect of mechanical deformation and heat treatment, including observing pre-existing aspects of the material.

3 Method

Aiming to study the behavior of the microstructure of Brass C260 during the mechanical forming process and also during annealing, properties such as hardness and grain size of the raw material and samples of the material were evaluated after each of the four stages of the fabrication route for an ammunition component. Based on the experimental results, an attempt was made to understand the relationship between the microstructure and the physical-mechanical properties of the alloy under study.

For the preparation of test specimens, five 70/30 brass blanks were selected, which are typically used as raw material in cartridge manufacturing. One blank was separated immediately, while the other four underwent cold deep drawing in a hydraulic press, followed by alkaline degreasing, after which one cup sample was extracted. The three remaining cups were then annealed in a trolley furnace and subsequently pickled, where another cup sample was taken. The two cups still remaining were cold-stretched in a hydraulic press, followed by alkaline degreasing; one more cup was removed, and the last underwent a second annealing in the same trolley furnace. The selected samples (cups and the blank) were coded for identification and their dimensions measured using a Mitutoyo digital caliper. Selected samples were sectioned to extract specimens for microhardness testing and metallographic analysis, according to relevant standards. The procedures for sampling and specimen preparation described above are illustrated in the flowchart in Figure 1.

Figure 1: Descriptive planning used in the work.

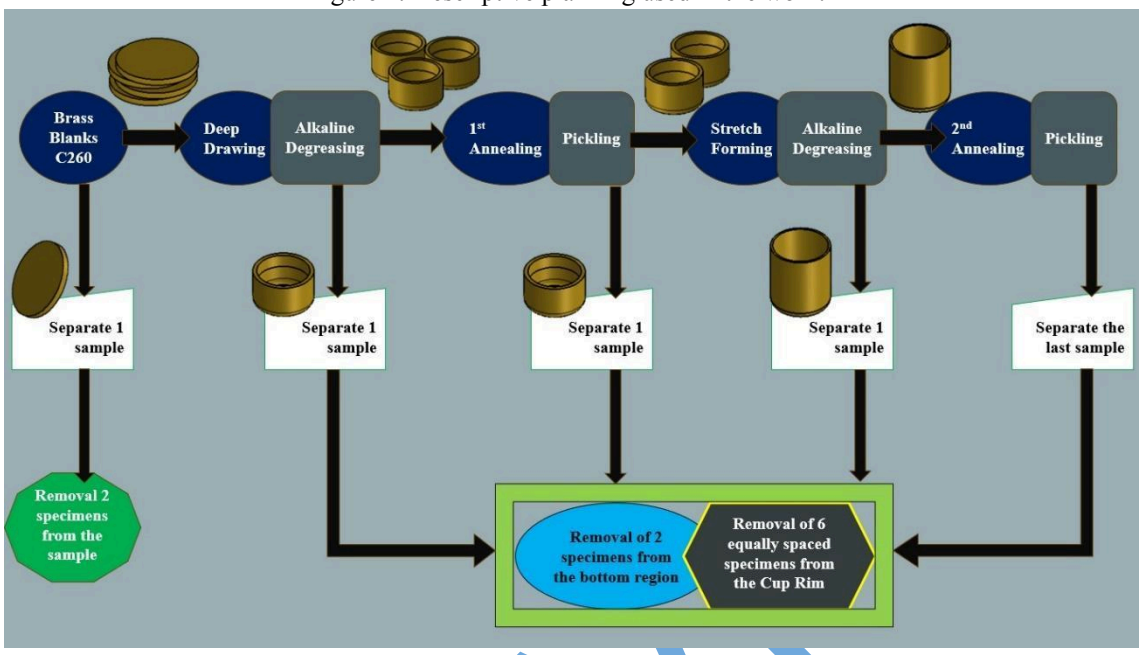

Source: Authors (2025).

The flowchart in figure 2 lists the experimental methods and analysis of the results.

Figure 2: Flowchart of the tests carried out.

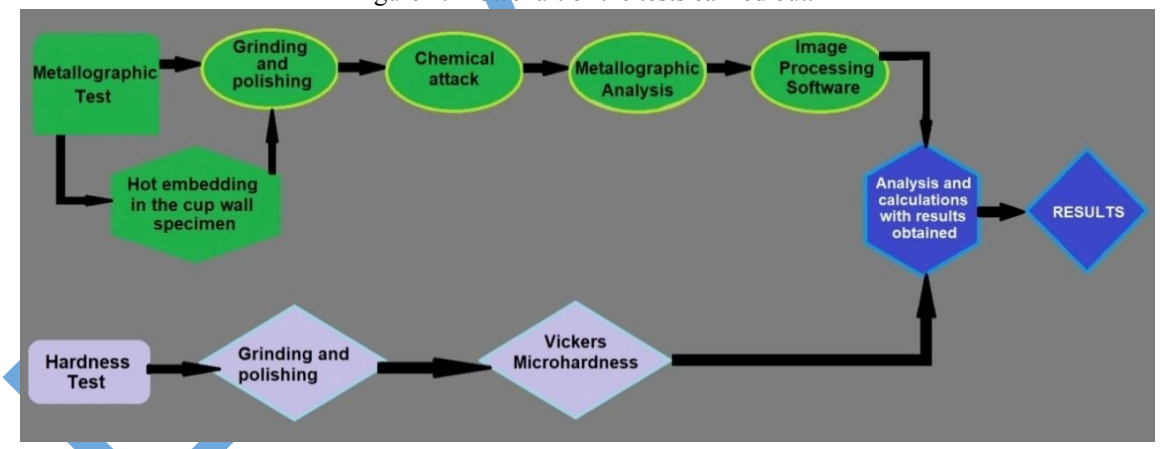

Source: Authors (2025).

The blanks underwent a Deep Drawing process in a hydraulic press with a capacity of 2200 tf from the Hidralmac brand. Drawing tallow was used as a lubricant on the surface of the punch as well as on the blank. The cups subjected to alkaline degreasing, were subsequently annealed in a Jung trolley oven, where they were heated along with the furnace for approximately 1 hour until reaching 600 °C. They were held at this temperature for 25 minutes, then removed from the oven and left cooling in the air inside the still hot wagon. Subsequently, the cups were pickled and subjected to stretching in a hydraulic press with a capacity of 150 tf from the Hidralmac brand. Tallow was used for drawing as a lubricant on the surface of the punch as well as on the inside and outside of the cup.

After cleaning, they underwent annealing in a Jung trolley oven, where they were heated together with the oven for approximately 30 minutes until reaching a temperature of 550 °C where they remained for 20 minutes and then were removed from the oven and left to cool in the air inside the still hot wagon.

Figure 3 shows the preparation of the specimens obtained from the blanks. Two specimens were taken from the sample, a small square with a side of 20 mm to carry out the metallography (3a) and another square with a side of 30 mm to obtain the hardness profile (3b).

Figure 3: Test specimens originating from blanks (a) Metallography; (b) Microhardness.

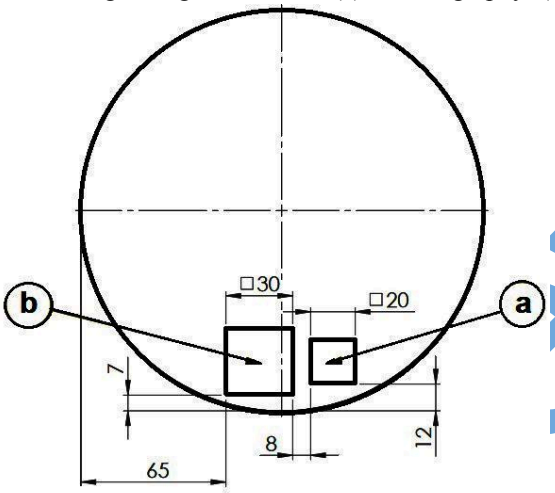

Source: Authors (2025).

Subsequently, two specimens were removed from the cup bottom region (figure 4 a), a small square with a side of 20 mm to carry out the metallography and another square with a side of 30 mm to obtain the hardness profile. Finally, six equally spaced specimens with a width of 20 mm were removed from the rim of the cup (wall), one for metallography and the others for obtaining the hardness profile, as shown in figure 4 b. It should be noted that there is a difference in the height of the cups due to the processing steps, so it was adopted that the region where these last specimens were removed has its lower limit 25 mm from the lowest point of the edge of the cup.

Figure 4: Sample sections (a) Bottom region (b) Wall Region.

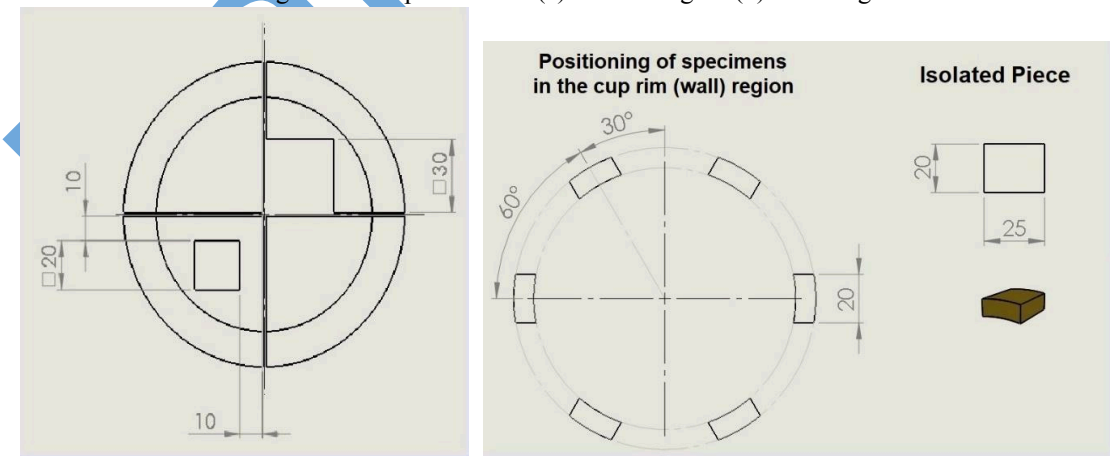

Source: Authors (2025).

The metallographic preparation was carried out according to the procedures recommended by ASTM E3-11 (2017) as follows: hot mounting in a Fortel brand press, model EFD 30, applied only to

the samples taken from the cup walls. Afterwards, grinding was performed together with the other specimens in the following sequence of 80, 600, 800, 1200 and 1500 mesh sandpapers, followed by polishing on felt cloth with diamond pastes of 3 and 1 µm grain size, and final finishing with 0.3 µm alumina. A Teclago metallographic grinder, model PL02 ED, and a double polisher, Arotec, model PL 02, were used for the grinding and polishing operations. The specimens were also washed with 99% isopropyl alcohol and dried with a jet of heated air, before being etched for 3 seconds with 100% Nitric acid (HNO_3) using a cotton pad.

In order to analyze the respective grain sizes, the linear intersection method or Heyn was applied, according to the ASTM E112-10 standard with the ImageJ software. The total length of the test lines divided by the count result was adopted as the average grain size. Subsequently, this value was used to calculate the ASTM grain size (G), according to Equation 1.

$$G = \left(6,643856.log\left(P_L\right)\right) - 3,288 \quad (1)$$

Where:

P_L: number of grain boundary intersections per unit of test line length, in mm^{-1} according to ASTM E112 (2010).

The results obtained also underwent a Shapiro-Wilk test using the PAST statistics software in order to assess whether the data distribution was a normal or Gaussian distribution for the purpose of comparing the means. Subsequently, a comparison was made between the average grain sizes through the Tukey's Test, this time using the R_{studio} software. The purpose of this test is to identify how significant a change in grain size may have been between one operation and another.

For the metallographic test, the samples were grinded in the following sequence of 80, 600, 1500 mesh sandpaper, polishing on felt cloth with 1-µm alumina. A Teclago metallographic sander, model PL02 ED, and a double polisher, Arotec, model PL 02, were used for grinding and polishing operations. The pieces were also washed with 99° isopropyl alcohol and dried in a jet of heated air, being subsequently tested in a Vickers Digital Microhardness Tester, Shimadzu, model HMV - G 21 ST, with a load of 0.2 kgf, penetration for 5 seconds and magnification of 40 times.

Five penetrations were made in the specimens from the blank and the bottom region (Figure 5 a) and 1 penetration in each of the five squares on the edge of the cup (Figure 5 b). Figure 5 shows the reference measurements for the penetrations, in both cases. In order to improve the support during the execution of the test of these wall hardness, in view of the shape of the specimen, a base made of high hardness steel (AISI H13) with a radius matching that of punch used to form the inner diameter of the cups was employed.

Figure 5: Distribution of Hardness test Indentations: (a) Bottom region and Blank; (b) Wall region.

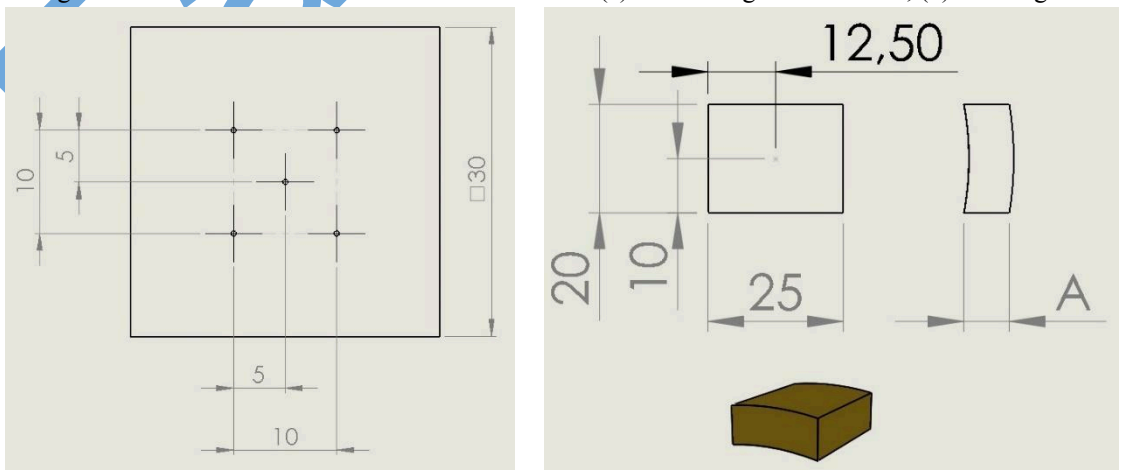

Source: Authors (2025).

4 Results and discussion

Figure 6 shows a diagram of the dimensions obtained using a digital caliper and Table 1 complements the values step by step for the cup-shaped samples.

Figure 6: Sample Dimensions – a) Blank; b) Cup shape.

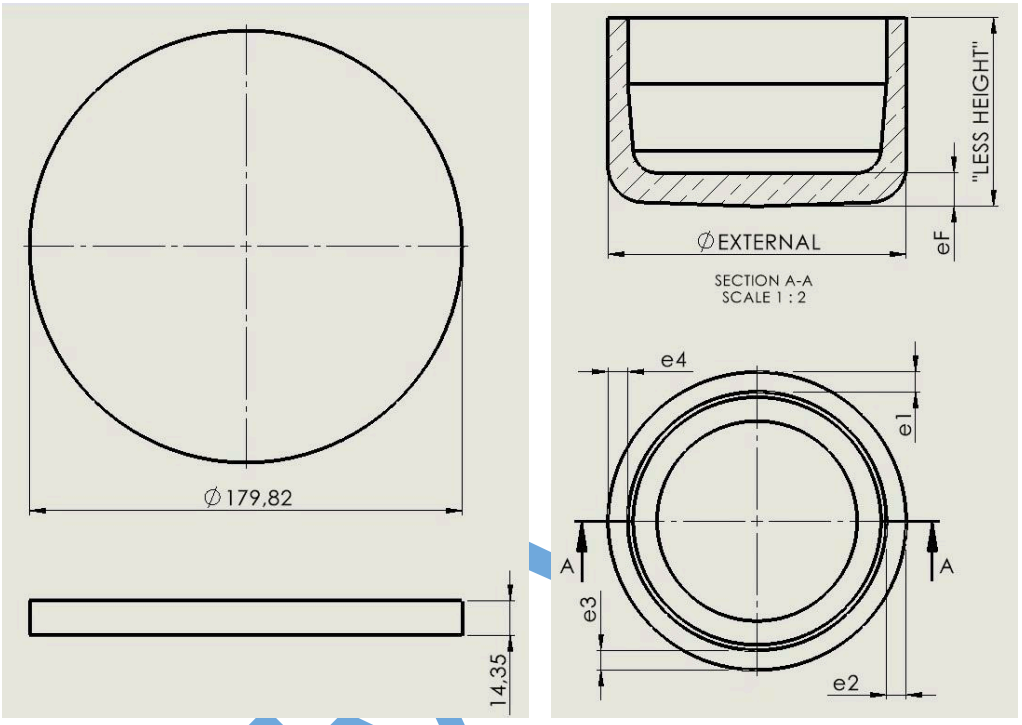

Source: Authors (2025).

Table 1: Table Dimensions in mm of the cup-shaped samples.

Operation	Thickness (e) (mm)						Ø External (mm)	Lesser height (mm)
	e1	e2	e3	e4	Av.	eF		
Deep Drawing	8.8	8.3	8.6	8.6	8.6	14.10	124.8	80.5
1st Annealing	8.4	8.4	8.4	8.5	8.4	14.15	124.85	80.2
Stretch forming	4.5	4.7	4.9	4.5	4.7	14.08	117.05	140.2
2nd Annealing	4.4	4.4	4.5	4.5	4.5	14.10	117.05	143.2

Source: Authors (2025).

Based on these values, it was possible to calculate the percentage of cold work (%CW) of each stage, through Equation 2, thus generating Table 2.

$$\%CW = \left(\frac{A_0 - A}{A_0}\right) X100 \qquad (2)$$

Where:

A_0: Initial cross-sectional area;

A: Final cross-sectional area.

The deep drawing die comprises two sequential rings. The design parameters of the first ring were utilized in the calculations, as measuring the cup immediately after passing through this ring is not feasible. Therefore, the post-deep drawing cold work percentage (%CW) is the sum of both rings. The external radius (R_{ex}) and average values for the second ring, as well as for the stretching, are derived from the mean dimensional measurements of the cups that were hardened and immediately annealed after each operation.

Table 2: Percentage of cold work for each stage of the process.

Operation		R external (mm)	R internal (mm)	E avg (mm)	Area (mm²)	Cold work (% CW)
Blank		89.91	-	14.35	7459.69	-
Deep Drawing	1st ring	65.00	54.07	10.93	4088.58	45.19
	2nd ring	62.41	53.91	8.50	3106.29	24.03
Stretch forming		58.53	53.98	4.60	1608.10	48.23

Source: Authors (2025).

It can be noted that the deep drawing operation yields the highest cold work percentage.

Micrographs at 100× magnification (Figures 7 and 8) disclose the α-phase matrix of the brass and confirm the presence of mechanical or annealing twins in all samples. This is consistent with predictions by Humphreys & Hatherly (2004) and Birch et al. (2024) for materials possessing low stacking fault energy.

Figure 7: Micrograph of the C260 brass blank.

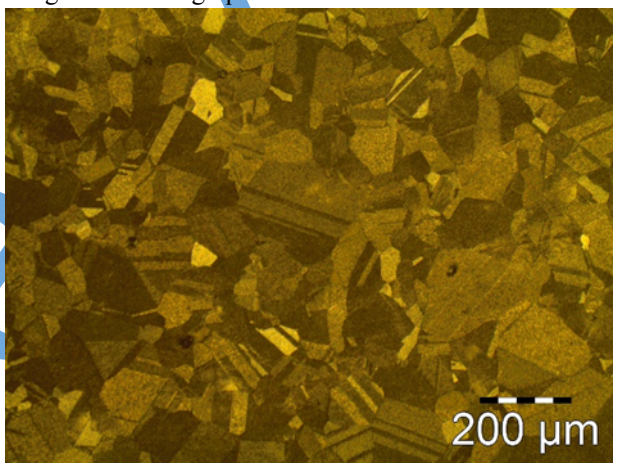

Source: Authors (2025).

The Blank micrograph (Figure 7) demonstrates a predominance of equiaxed grains, that is, without an orientation preference or texture that could lead to anisotropic behavior and bring defects to stamping processes such as wall thinning or earing. Based on this analysis, it is possible to state that the technical requirements of the blank (rolled and annealed) were met since new grains were nucleated through the recrystallization process. Figure 8 represents the stages deformed in a cup shape, with 8a, 8c, 8e and 8g the bottom regions and 8b, 8d, 8f and 8h the wall regions.

Figure 8: Micrograph of the C260 brass samples, 8a, 8c, 8e and 8g the bottom regions and 8b, 8d, 8f and 8h the wall regions.

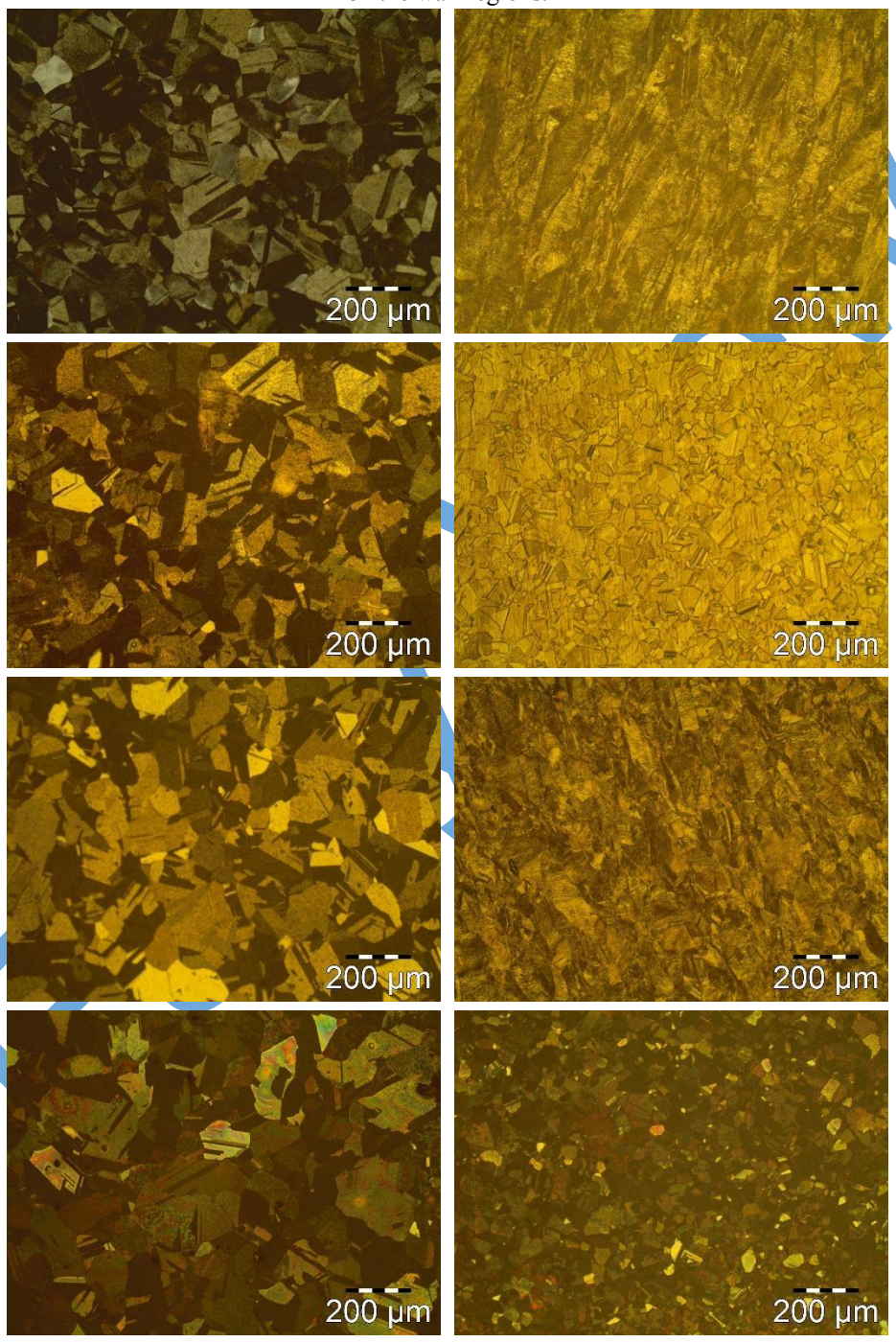

Source: Authors (2025).

No significant changes were observed in the bottom regions; their microstructure remains similar to that of the original blank. This was expected, given the minimal dimensional change in that area, which indicates negligible mechanical deformation. On the other hand, the wall regions display evident microstructural evolution during forming, distinguishing them from the original blank. In Figures 8b and 8f, elongated grains with corrugated boundaries and intersecting slip bands, typical features of cold strain hardening, are observed. Ozgowicz (2010) reported similar microstructural features in rolled C260 brass with reductions between 15.8% and 70.2%. Crystallographic texture development is also evident, arising from the alignment of the crystallographic axes relative to the macroscopic deformation directions.

The metallographic analysis referring to the thermal annealing treatments (Figures 8 d and 8 h) show smaller isomorphic grains that make it possible to state that there was a significant recrystallization with grains migrating to high angle contours as a result of a diffusion process at high temperatures. Klein (2016), when working with 70/30 brass with different %CW and also different annealing times and temperatures, found similar microstructures with variables similar to that of this work and attributed the small grains to the high cold deformation index. Ozgowicz (2010) also found such a relationship in his work.

The grain size of the blank and of the samples submitted to the thermomechanical processes presented a Gaussian distribution, which made it possible to apply the Tukey test to compare their average grains, with the aid of the Rstudio software. Table 3 represents the mean grain size values obtained by the Heyn linear intercept method (LIM), along with the corresponding ASTM grain size number (G).

Table 3: Average Grain Size and G (ASTM) values.

Operation	**Bottom Region**		**Wall Region**	
	λ (μm)	**G (ASTM)**	**λ (μm)**	**G (ASTM)**
Blank	47.36	5	47.36	5
Deep Drawing	53.27	5	52.06	5
1st Annealing	51.01	5	26.32	7
Stretch forming	44.88	6	44.21	6
2nd Annealing	53.27	5	31.07	7

Source: Authors (2025).

The average grain values referring to the bottom region show slight changes in grain sizes during the sequence of operations which, after being compared by Tukey's test, proved to be insignificant for a confidence level of 95%. Regarding the annealing steps, the insignificance of alteration confirms the first law of recrystallization, which states that a minimum degree of deformation is necessary for it to occur, considering that the energy stored in the material is important to sustain the growth of a nucleus. Klein (2016) did not observe significant changes in the grain structure when annealing a brass without initial deformation for 60 min at 425 °C.

According to Tukey's test, the grain size changes in the wall region after deep drawing and stretching were significant, which is consistent with the high degree of cold work imposed during these operations. It should be clarified that this reduction is not grain coarsening but the formation of a new deformation-induced microstructure, typical of low stacking-fault-energy materials in which mechanical twinning and dislocation glide elongate grains and produce parallel slip bands. Ozgowicz (2010) reported similar microstructures in rolled C260 brass with approximately 42.5% reduction. Likewise, recent studies employing strain-gradient samples confirmed that cold-worked α-brass exhibited comparable features under subsequent heat treatment (Birchall & Bishop, 2025). Birch et al. (2024) obtained closely related results for the same alloy.

Observations of grain size in the wall region after annealing (1st and 2nd) indicate a significant decrease, as confirmed by Tukey's test. This suggests that the annealing process provided sufficient thermal energy to facilitate dislocation movement, relieve deformation-induced stresses, and promote the nucleation of new grains. Klein (2016) investigated the effects of variables such as %CW, temperature, and time on the recrystallization behavior of C260 brass. He found that during recrystallization, the material's microstructure resembles its pre-worked state in shape, with grain size varying depending on these factors. Similar findings were reported by Moreira et al. (2023) and Nascimento et al. (2023).

Another interesting observation is that the smallest grain size occurs after primary annealing (1st) following the operation with the highest percentage of cold work (deep drawing) and also when compared to stretching, as confirmed by Tukey's test, indicating a highly significant change. This aligns with the 4th law of recrystallization, which states that a higher degree of deformation produces smaller recrystallized grains, since more intense deformation generates more nuclei per unit volume, resulting in a smaller average grain size (Humphreys, Hatherly, 2004). Aniceto et al. (2016) evaluated C260 brass laminated from an initial to a final thickness through two pass schedules and observed that the sample with fewer rolling passes exhibited higher nucleation intensity during recrystallization under the same temperature and annealing time, producing a smaller average grain size compared to the sample with more passes. Figure 9 shows the microhardness measurements along the test specimens.

Figure 9: Evolution of Vickers microhardness during the manufacturing process.

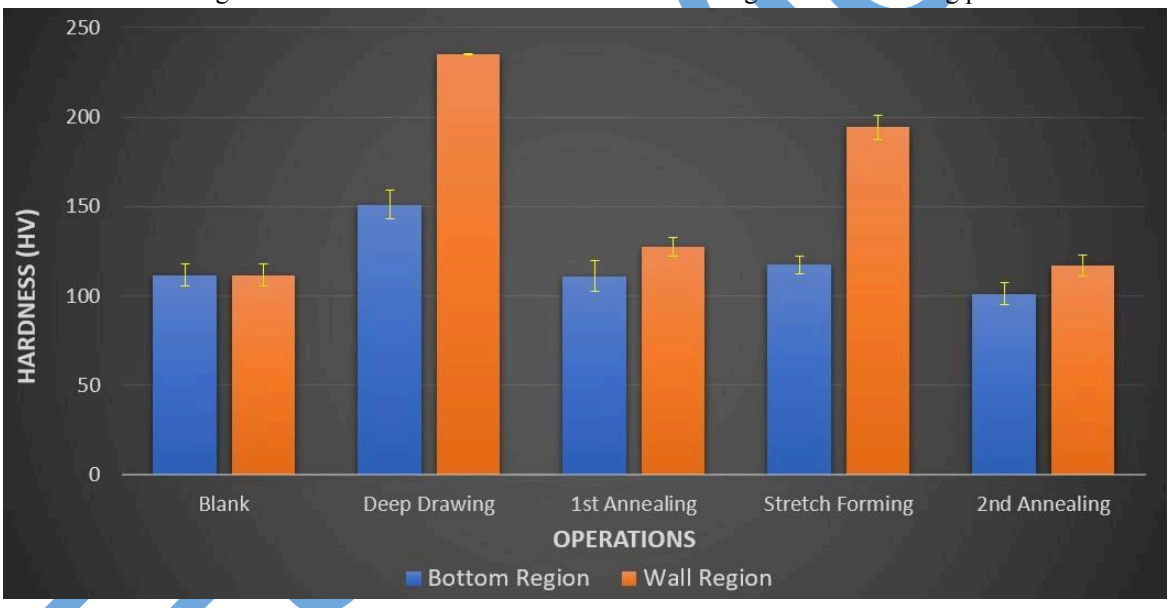

Source: Authors (2025).

Just as the grain size was analyzed, the hardness profile of the bottom region shows little variation across the stages. Although increases in hardness were observed after deformation operations and decreases after annealing, the differences between consecutive steps remain small. The only value that stands out to a greater extent is that of the post-blanking specimen, which exhibits the highest hardness in this region. This behavior was expected, considering that, although there is a minimal change in thickness at the bottom region, there is a visible geometric modification when comparing the curvature radius of the blank with that of the bottom after the operation. Brooks (1982) explains that metals with low stacking fault energy exhibit low dislocation mobility, a condition that significantly reduces the occurrence of climb and cross-slip phenomena. Moreira (2015) also emphasizes their effect on dislocation distribution, supporting the fact that alloys with low stacking fault energy, such as

brass, tend to accumulate a higher dislocation density, which facilitates hardening and consequently increases material hardness.

Souza (2014) observed that cold-rolled C26800 brass and C12000 copper exhibited different work hardening behaviors. Brass showed an 80% increase in hardness, while copper showed a 60% increase. Notably, after 30% deformation, copper's hardening rate decreased, whereas brass maintained a more consistent hardening rate. These differences are attributed to the materials' stacking fault energy (SFE): brass has a lower SFE, leading to more uniform dislocation distribution and less dynamic recovery, while copper's higher SFE allows for more dynamic recovery and less dislocation accumulation.

The characteristics discussed above are also observed in the wall region, intensified by the higher %CW, which causes significant variations to occur in its hardness profile that follow the logic already seen in the grain size analysis of this region with increases in hardness in post-forming mechanical operations such as deep drawing and stretching, that is, in hardened materials. Values such as 142 HV for a cold rolling reduction of 15.8% and 212 HV for 70.2% were found by Ozgowiks (2010) when working with the same alloy, in accordance with the tests with a view to the highest value of hardness found to be 235 HV in deep stamping while 194 HV in drawing. The hardness behavior also reduced with the recrystallization of the materials, that is, after the respective annealings. This drop in hardness after heat treatment was also consistent with the observations of Mutlu et al. (2023), in whose study the hardness of the formed material progressively decreased with increasing recrystallization temperature, approaching the initial values at 550°C.

Note that the hardness between annealings has similar values if the respective standard deviations are considered. This fact is also demonstrated in the comparison of the respective grain sizes, which presented an insignificant difference. The 5th law of recrystallization states that to complete a recrystallization at the same time and temperature with a larger initial grain, a larger %CW is required. Therefore, the high %CW value in the deep drawing after a larger blank grain size against a lower %CW value in a smaller grain size (from 47.36 µm in the blank to 26.32 µm in the 1st annealing). Such a law could explain such close hardness, but for that it would be necessary to study the kinetics of the recrystallization of the material under these deformation conditions. The grain sizes obtained in the wall annealing's were significantly lower than those found in the blank, possibly due to the high %CW value of the respective forming steps preceding the heat treatments. Consequently, the hardness values after annealing, despite having been reduced in relation to their respective conformations with efficiency, are still higher than those of the blank.

Another fact observed about these hardnesses in the wall region after annealing is which are superior to the background regions of the same samples even considering the deviations standards. There is a large grain size difference between these regions in the same samples, which can be explained by the first law of recrystallization. Therefore, the grain sizes of the wall samples in question are smaller than those of the respective background regions, which explains their superior hardness. Barbosa (2018) observed this relationship between grain size and hardness when evaluating 70/30 brass after annealing heat treatment. A decrease in hardness with increasing grain size was also reported by Muhammed et al. (2012) when studying the effects of recrystallization temperature on the mechanical properties of the same alloy. Birch et al. (2024 also reported similar hardening behavior in cold-worked α-brass subjected to heat treatment).

5 Conclusions

The annealing revealed differences between the bottom and wall regions. The bottom regions exhibited minimal microstructural variation and hardness, similar to the initial material, indicating

insufficient cold work for recrystallization. In contrast, the wall regions underwent effective recrystallization during both annealing stages, forming significantly smaller equiaxed grains and reducing hardness. The smallest grain size was observed after the first annealing, highlighting the importance of the initial cold work percentage (%CW) in determining the final grain size. This suggests that the %CW during the blank's rolling was lower than in subsequent forming operations, as the annealed grains were notably smaller than those in the original blank. Consequently, the hardness of the annealed material was higher than that of the blank.

The blank exhibited an equiaxed microstructure without preferential grain orientation, confirming the effectiveness of the supplier's post-rolling annealing in preventing anisotropic behavior, such as hearing. This was corroborated by the absence of such defects during sample collection. Comparisons among the annealed materials showed negligible variation in grain size and very similar hardness values, emphasizing the importance of initial grain size on final material properties.

A study on the thermal cycles of C260 brass, from the perspective of recrystallization kinetics, would be necessary to deepen the understanding of this effect, particularly because the annealing temperatures and dwell times differ between stages. In addition, such a study could support proposals to optimize the process under investigation.

5.1 Study limitations and future perspectives

Limitations:

- Dependence on a pre-existing industrial route: the work represents a section of an already consolidated manufacturing process, which made it impossible to modify certain process variables, such as the percentage of cold work.
- Restriction to the use of existing dies: the dies employed in forming were pre-existing and could not be replaced, either due to the high manufacturing cost or the need to maintain fidelity to the actual industrial process.
- Limitation regarding the alloy: the C260 brass (70/30) is the established material for cartridge manufacturing, which prevented its comparison with alternative alloys in this study.
- High material cost: the considerable value of brass limited the acquisition of a larger number of samples, restricting the experimental scope.

Future Perspectives:

- Expansion of the experimental base: seek institutional or industrial partnerships to enable greater material availability, allowing for a broader set of tests.
- Conduct studies on the recrystallization kinetics of C260 brass under different levels of cold deformation and annealing conditions (time/temperature), aiming to model the mechanisms of grain nucleation and growth;
- Employ advanced characterization techniques (MEV, EBSD, TEM) to map crystallographic texture, twin distribution, and low/high-angle grain boundaries, enabling the correlation between microstructure and mechanical properties on a more detailed scale;
- Perform computational simulations of the alloy behavior under forming and annealing routes, in order to predict microstructural evolution and optimize industrial processes.

Nota:

Os resultados deste trabalho são decorrentes do trabalho de conclusão de curso de Douglas Luiz da Cruz, no Bacharelado em Engenharia Metalúrgica do Instituto Educação, Ciência e Tecnologia do Sudeste de Minas Gerais – Campus Juiz de Fora (IF SUDESTE MG), disponível em: https://drive.google.com/file/d/1qQ9qpMYpQrypBNSYtqABpJ_B08MXKkKU/view?usp=sharing

Contribuições ao artigo:

CRUZ, D. L.: Concepção ou desenho do estudo/pesquisa; Coleta, análise e/ou interpretação dos dados; Elaboração e redação do manuscrito;

OLIVEIRA, M. J. C.: Elaboração e redação do manuscrito; Revisão crítica, com participação intelectual significativa; Supervisão geral e coordenação do projeto ou estudo;

MEINHARDT, C. P.: Revisão crítica, com participação intelectual significativa;

References

ANICETO, P. J. *et al.*Avaliação da influência do caminho de laminação no tamanho de grão final. *In:* **53° Seminário de Laminação, 2016**, Rio de Janeiro. Anais [...], Rio de Janeiro: ABM, 2016. p.340-347.

BARBOSA, C. **Metais não ferrosos e suas ligas: microestruturas, propriedades e aplicações**. Rio de Janeiro: E-papers, 2014.

BARBOSA, C. Avaliação das características microestruturais da liga cobre-30%zinco após tratamento térmico. *In*: ***73º Congresso Anual da ABM*, 2018, São Paulo, Anais** [...], São Paulo: ABM, 2018. p. 21-30.

BIRCH, J. *et al*. A micromechanical study of heat treatment induced hardening in α-brass. **Acta Materialia**, v. 278, p. 120277, 2024. doi.org/10.1016/j.actamat.2024.120277

BIRCHALL, F., BISHOP, C. High-Throughput Quantification of Recrystallization Parameters for Alloy Development. **Metallurgical and Materials Transactions A**, v. 56, n. 8, p. 3095-3110, 2025. DOI: 10.1007/s11661-025-07822-4.

BROOKS, C.R. **Heat treatment, structure and properties of nonferrous alloys**. Ohio: ASM, Metals Park, 1982.

GRIGORAS, C. C. *et al.* Machine Learning, Mechatronics, and Stretch Forming: A History of Innovation in Manufacturing Engineering. **Machines**, V. 12, p. 180, 2024. doi.org/10.3390/machines12030180

HIRT, G. *et al.* Flexible cnc incremental sheet forming: process evaluation and simulation. **Institute of Materials Technology/Precision Forming (LWP)**, Saarland University, Germany, p. 12, 2005.

HUMPHREYS, F. J.; HATHERLY, M. **Recrystallization and related annealing phenomena**. 2. ed. Oxford: Elsevier, 2004.

KLEIN, J.; INDACOCHEA, J. Recrystallization Behavior of 70/30 Brass. University of Illinois at Chicago CME 470 **Physical and Mechanical properties of materials**. *[s.l: s.n.]*, 2016.

MERAYO, D., PRIETO, A. R., CAMACHO, A. M. Topological Optimization of Artificial Neural Networks to Estimate Mechanical Properties in Metal Forming Using Machine Learning. **Metals**, v. 11, p. 1289, 2021. doi.org/10.3390/met11081289

MOREIRA, C. E. S.; CRUZ, D. L.; OLIVEIRA, M. J. C. Aplicação do planejamento fatorial e análise de superfície de resposta no processo de recristalização da liga C260 após estiramento. In. **76º**

Congresso Anual da ABM – Internacional, 2023, São Paulo. Anais do 76º Congresso Anual da ABM – Internacional, 2023. doi.org/10.5151/2594-5327-39612

MOREIRA, V. C. Efeito do teor residual de Fe no recozimento do latão 70/30. 2015. **Dissertação (Mestrado em Engenharia Metalúrgica e de Materiais)** - Departamento de Engenharia Metalúrgica e de Materiais, Escola Politécnica da Universidade de São Paulo, São Paulo, 2015.

MUHAMMED, A.; ABED, A.; MUSTAFA, M. A. Effects of recrystallization temperature on the mechanical properties of CuZn30 alloy. In: THE FIRST NATIONAL CONFERENCE FOR ENGINEERING SCIENCES, 2012, Baghdad. **Proceedings of The First National Conference for Engineering Sciences**. Baghdad: IEEE, 2012. p. 1-6. DOI: 10.1109/NCES.2012.6740482.

MUTLU, M. *et al*. Flow forming and recrystallization behaviour of CuZn30 alloy. In: INTERNATIONAL ESAFORM CONFERENCE ON MATERIAL FORMING, 26., 2023, Kraków. **Material Forming**. Millersville, PA: Materials Research Forum, 2023. p. 1021-1028. DOI: 10.21741/9781644902479-112

NASCIMENTO, M. V. S.; CRUZ, D. L.; OLIVEIRA, M. J. C. Análise microestrutural e das propriedades mecânicas da liga de latão 70/30 recozida após embutimento. In: **76º Congresso Anual da ABM – Internacional**, 2023, São Paulo. Anais do 76º Congresso Anual da ABM – Internacional, 2023. doi.org/10.5151/2594-5327-39623

OZGOWICZ, W.; KALINOWSKA-OZGOWICZ, E.; GRZEGORCZYK, B. The microstructure and mechanical properties of the alloy CuZn30 after recrystallization annealing. **Journal of achievement in materials and manufacturing Engineering**, Gliwice, v. 40, n. 1, p. 15-25, 2010.

SOUZA, T.G. Avaliação de densidade de discordâncias em cobre e latão α deformados por análise de largura de pico de DRX. 2014. Dissertação (**Mestrado em Ciência dos Materiais**) – Instituto Militar de Engenharia. Rio de Janeiro, 2014.